International Journal of Chemical Science
www.chemicaljournals.com
Online ISSN: 2523-2843
Received: 01-03-2026, Accepted: 02-04-2026, Published: 16-04-2026
Volume 10, Issue 2, 2026, Page No. 24-30

Synthesis, crystal structure, and Hirshfeld surface analysis of 3,14-dimethyl-2,6,13,17-tetraazoniatricyclo(16.4.0.0^{7,12})docosane tetranitrate dihydrate

Dohyun Moon[1], Jong-Ha Choi[2*]
[1] Department of Pohang Accelerator Laboratory, Postech, Pohang, South Korea
[2] Department of Chemical and Biological Engineering, Gyeongkuk National University, Andong, South Korea

Abstract
A novel compound, $[C_{20}H_{44}N_4](NO_3)_4{\cdot}2H_2O$ (1), was synthesized and characterized by single-crystal X-ray diffraction as well as elemental analysis. The structure determination reveals that protonation has occurred at all four N atoms of the amine. The asymmetric unit contains one macrocyclic tetracation, four nitrate anions and two water molecules. The organic $[C_{20}H_{44}N_4]^{4+}$ fragment of 1 adopts an exodentate (3,4,3,4)-*A* conformation. The N–C and C–C bond lengths of the macrocyclic tetracation range 1.500(3) – 1.522(3) Å and 1.517(3) – 1.541(3) Å, respectively. A three-dimensional hydrogen bonding network provides crystal cohesion through N–H···O, O–H···O, and C–H···O interactions between organic cations, nitrate anions, and water molecules. The Hirshfeld surface analysis and 2D fingerprint plots reveal that the crystal packing in 1 is primary dominated by O···H/H···O, H···H, and N···H/H···N contacts.

Keywords: Crystal structure, tetraprotonated macrocycle, exodentate, (3,4,3,4)-*A* conformation, Hirshfeld surface analysis

Introduction

In recent years, compounds containing the 14-membered macrocyclic cyclam (1,4,8,11-tetraazacyclotetradecane) and cyclam derivatives have been shown to exhibit potential inhibitory effect on human immunodeficiency virus (HIV) replication and the ability to mobilize hematopoietic progenitor stem cells from the bone marrow into the blood. Information about the conformation and crystal packing forces of cyclam derivatives is essential for developing new anti-HIV drugs because these structural features directly influence the drug's ability to bind to its biological target, primarily the CXCR4 co-receptor, and affect its overall pharmacological properties.

The macrocycle 3,14-dimethyl-2,6,13,17 tetraazatricyclo(16.4.0.0^{7,12})docosane ($C_{20}H_{40}N_4$, L) contains a cyclam backbone with two cyclohexane subunits and two methyl groups located at the alpha positions on the propyl chain. Macrocycle L is a basic amine capable of forming the dication $[C_{20}H_{42}N_4]^{2+}$ ($[H_2L]^{2+}$) or tetracation $[C_{20}H_{44}N_4]^{4+}$ ($[H_4L]^{4+}$), in which all the N–H bonds are generally available for hydrogen bonding. The conformations of the macrocycle L and its protonated forms are governed by molecular hydrogen bonds and the degree of protonation. The neutral L ligand and the L^{2+} dication adopt an endodentate conformation (nitrogens oriented towards the macrocyclic cavity center) due to the stabilization provided by strong molecular hydrogen bonds. In contrast, the L^{4+} tetracation adopts an exodentate conformation (nitrogens oriented outwards). This change in conformation is likely due to the repulsion between the positively charged nitrogen atoms, which outweighs the stabilizing effect of the molecular hydrogen bonds, forcing the structure to open up. Additionally, the four exodentate (3,4,3,4)-(A~D) conformations of the 14-membered cyclam moiety are different spatial arrangements of the macrocycle, specifically in its tetraprotonated form, that are adopted depending on intermolecular interactions, primarily with counter-anions and solvent molecules. The nomenclature uses a series of numbers (3,4,3,4) to indicate the number of bonds between these corners in the macrocycle ring, which forms a diamond-lattice type structure [6.7]. The letters A, B, C, and D then differentiate the specific spatial configuration as shown in Fig. 1.

< Figure 1>

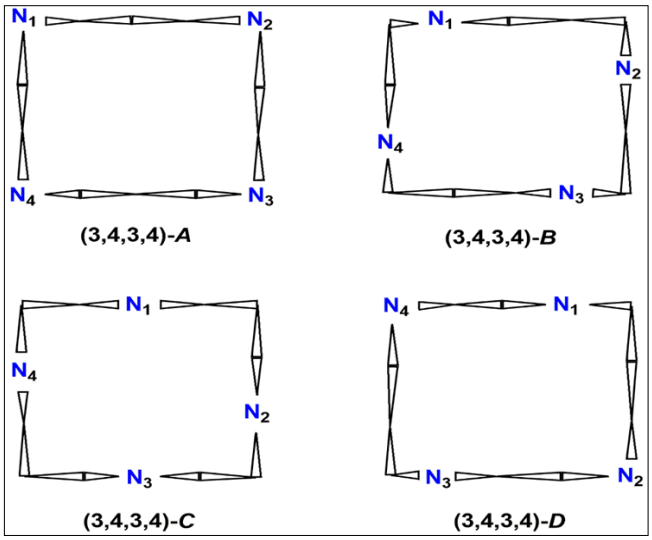

Fig 1: Four possible exodentate conformations of tetracationic cyclam moiety

The synthetic methods and their crystal structures of $(L){\cdot}2(C_{10}H_7CH_2OH)$, $(L){\cdot}2(NO_2OH)$, $[H_2L](SO_4){\cdot}2MeOH$, $[H_2L](ClO_4)_2$, $[H_2L]Br_2{\cdot}2H_2O$, $[H_4L]Br_4{\cdot}4H_2O$ and $[H_4L]Cl_4{\cdot}4H_2O$ have been reported. However, any salt of dication $[H_2L]^{2+}$ or tetracation $[H_4L]^{4+}$ with nitrate anions was not known until now.

In this paper, we describe synthesis of a new tetracationic compound, $[H_4L](NO_3)_4{\cdot}2H_2O$, (1) (Scheme 1) and its structural characterization by synchrotron single-crystal X-ray diffraction. Hirshfeld surface analysis was also performed to identify the main intermolecular contacts in the crystal packing.

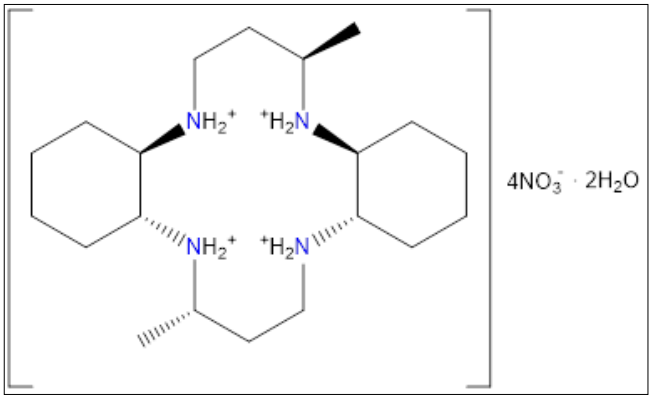

Scheme 1: Chemical structure of 1

Materials and method

1. Synthesis and crystallization

Commercially available trans-1,2-cyclohexanediamine (99%) and methyl vinyl ketone (97%) (Sigma-Aldrich) were used as provided. All chemicals were reagent grade and used without further purification. The macrocycle 3,14-dimethyl-2,6,13,17-tetraazatricyclo(16.4.0.0^{7,12})docosane was prepared according to previously published method. A solution of the macrocycle (0.036 g, 0.1 mmol) in water 20 mL was refluxed for 1 hour. After cooling to 298 K, 2 mL of HNO_3 was added to adjust the pH to 3.0. The solution was filtered, and left at room temperature. After a few days, colorless crystals suitable for X-ray analysis were obtained. Yield: 47%. Elemental Analysis. Calculated for $C_{20}H_{48}N_8O_{14}$: C, 38.46; H, 7.75; N, 17.94%. Found: C, 38.33; H, 7.74; N, 17.84%.

2. Physical measurement

Analyses for C, H, and N were performed on a Carlo Erba 1108 Elemental Vario EL analyzer.

3. Crystal structure analysis

The block-shaped colorless crystal of 1 with approximate dimensions 0.125×0.119×0.107 mm^3 was coated with Parabar 10312 (Hampton Research Inc.) to mount a micro-loop. The X-ray diffraction data were measured using a Rayonix MX225HS detector at BL2D-SMC with a silicon (111) double-crystal monochromator (λ = 0.630 Å) at the Pohang Accelerator Laboratory, Korea, by using synchrotron radiation under a nitrogen cold stream (T = 217 K). The PAL BL2D-SMDC program was used for data collection, and the HKL3000sm software (Version 716.7) was used for cell refinement, reduction, and absorption correction. The structure was solved using the intrinsic phasing method in the SHELXT program and refined by full-matrix least-squares calculations using the SHELXL program. Molecular graphics were generated using DIAMOND-5. All non-hydrogen atoms were refined anisotropically. All C and N-bound H atoms in the complex were placed in geometrically idealized positions and constrained to ride on their parent atoms, with C–H distances of 0.97 – 0.99 Å, and with N–H distance of 0.90 Å with U_{iso}(H) values of 1.2 and 1.5U_{eq} of the parent atoms respectively. The O-bound H atoms of the structural water molecules were located in a difference Fourier map and refined isotropically, with the O–H and H–O–H distances restrained using DFIX and DANG constraint (0.92 and 1.52 Å), respectively. The crystallographic experimental data and refinement parameters are summarized in Table 1.
<Table 1>

Table 1: Crystallographic data and refinement parameters for 1

Parameter	Value
Chemical formula	$[C_{20}H_{44}N_4](NO_3)_4{\cdot}2H_2O$
Empirical formula	$C_{20}H_{48}N_8O_{14}$
Formula weight	624.66
Temperature	217(2) K
Wavelength	0.630 Å
Crystal system, space group	Monoclinic, $P2_1$
Unit cell dimensions	a = 11.422(2) Å, α = 90°. b = 11.254(2) Å, β = 114.53(3)°. c = 12.774(3) Å, γ = 90°.
Volume	1493.8(6) Å3
Z	2
Density (calculated)	1.389 Mg m-3
Absorption coefficient	0.089 mm-1
F(000)	672
Crystal size	0.125 × 0.119 × 0.107 mm^3
Theta range for data collection	1.553 to 25.999°.
Reflections collected	15747
Independent reflections	8424 [R_{int} = 0.0598]
Completeness to θ = 22.210°	99.9%
Absorption correction	Empirical
Max. and min. transmission	1.000 and 0.907
Refinement method	Full-matrix least-squares on F^2
Data / restraints / parameters	8424 / 7 / 394
Goodness-of-fit on F2	1.137
Final R indices [F2> 2σ(F2)]	R_1 = 0.0540, wR_2 = 0.1586
R indices (all data)	R_1 = 0.0590, wR_2 = 0.1621
Absolute structure parameter	-0.2(14)
Extinction coefficient	N/A
Largest diff. peak and hole	0.603 and -0.289 e.Å^{-3}

Results and discussions

1. Crystallography

Single-crystal X-ray diffraction analysis was performed to determine the exact conformation of 1 in the solid state. Compound 1 crystallizes in the monoclinic space group $P2_1$ with two mononuclear formula units in a cell of dimensions a = 11.422(2), b = 11.254(2), c = 12.774(3) Å, and α = 90, β = 114.53(3) and γ = 90°. A perspective view of 1 along with the atom numbering scheme is shown in Fig. 2.

< Figure 2>

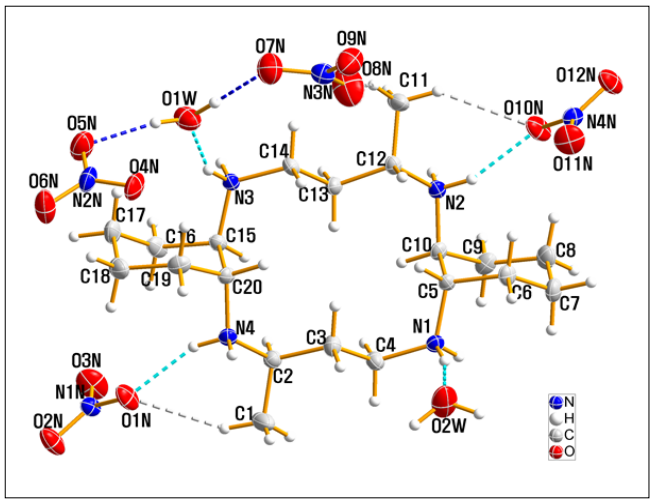

Fig 2: The molecular structure of 1, showing displacement ellipsoids drawn at the 30% probability level. Dashed lines represent hydrogen bonding interactions and primed atoms are related by the symmetry code (1-*x*, 1-*y*, 1-*z*)

The compound 1 is consisted of a positively charged macrocyclic tetracation, four NO_3^- counter anions and two solvent water molecules. The organic tetracation $[H_4L]^{4+}$ actually adopts an exodentate (3,4,3,4)-*A* conformation, where the four nitrogens in 14-membered cyclam moiety are located at the corners of the quadrangular macrocycle. The cyclam moiety within the tetracation folds in a way that directs the four nitrogen atoms outwards, making them face away from the macrocyclic cavity (exodentate), rather than towards the center (endodentate). This allows the nitrogen atoms to engage in intermolecular interactions, typically with NO_3^- counter anions and hydrate molecules, outside the ring. The exodentate rectangular conformation is notably different from the endodentate conformations of the neutral ligand and the dication unit seen in $(L)\cdot 2(C_{10}H_7CH_2OH)$, $(L)\cdot 2(NO_2OH)$, $[H_2L](SO_4)\cdot 2CH_3OH$, $[H_2L](ClO_4)_2$, $[H_2L]Br_2\cdot 2H_2O$. The *exo* (3,4,3,4)-*A* conformation of 1 is also distinct from *exo* (3,4,3,4)-*B* conformation of $[H_4TMC](CrO_3Cl)_2Cl_2$ (TMC = 1,4,8,11-tetramethyl-1,4,8,11-tetraazacyclotetradecane), *exo* (3,4,3,4)-*C* conformation of $[H_4TMC](ClO_4)_2Cl_2$ or $(H_4cyclam)[Cr_2O_7]_2\cdot H_2O$, and *exo* (3,4,3,4)-*D* conformation of $[H_4L]Br_4\cdot 4H_2O$ or $[H_4L]Cl_4\cdot 4H_2O$. All four alternative conformers for tetracation unit have the same *exo* conformation, but differ in the position of nitrogen atoms within the macrocyclic ring. Two six-membered cyclohexane ring of organic tetracation is in a stable chair conformation. Selected bond lengths and angles and their standard deviations for 1 are listed in Table 2. <Table 2>

Table 2: Selected bond lengths [Å] and angles [°] for 1

N1—C4	**1.507 (3)**	**C15—C20**	**1.541 (3)**
N1—C5	1.513 (3)	C16—C17	1.526 (4)
N2—C10	1.510 (3)	C17—C18	1.524 (4)
N2—C12	1.522 (3)	C18—C19	1.525 (4)
N3—C14	1.500 (3)	C19—C20	1.535 (3)
N3—C15	1.509 (3)	N1N—O3N	1.225 (3)
N4—C20	1.511 (3)	N1N—O1N	1.250 (3)
N4—C2	1.516 (3)	N1N—O2N	1.255 (3)
C1—C2	1.524 (4)	N2N—O4N	1.224 (3)
C2—C3	1.524 (3)	N2N—O5N	1.253 (4)
C3—C4	1.517 (3)	N2N—O6N	1.259 (4)
C5—C6	1.528 (3)	N3N—O8N	1.215 (4)
C5—C10	1.537 (3)	N3N—O9N	1.253 (3)
C6—C7	1.529 (4)	N3N—O7N	1.254 (4)
C7—C8	1.532 (4)	N4N—O11N	1.228 (3)
C8—C9	1.531 (4)	N4N—O12N	1.251 (3)
C9—C10	1.531 (3)	N4N—O10N	1.256 (3)
C11—C12	1.527 (3)	O1W—H1O1	0.917 (14)
C12—C13	1.521 (3)	O1W—H2O1	0.917 (14)
C13—C14	1.522 (3)	O2W—H1O2	0.904 (14)
C15—C16	1.528 (3)	O2W—H2O2	0.913 (14)
C4—N1—C5	117.94 (17)	N3—C15—C16	108.37 (19)
C10—N2—C12	119.78 (19)	N3—C15—C20	109.82 (17)
C14—N3—C15	118.00 (17)	C16—C15—C20	112.0 (2)
C20—N4—C2	118.91 (19)	C17—C16—C15	112.8 (2)
N4—C2—C3	110.63 (19)	C18—C17—C16	110.2 (2)
N4—C2—C1	107.7 (2)	C17—C18—C19	111.2 (2)
C3—C2—C1	112.0 (2)	C18—C19—C20	114.0 (2)
C4—C3—C2	109.08 (19)	N4—C20—C19	108.49 (19)
N1—C4—C3	112.77 (19)	N4—C20—C15	110.27 (18)
N1—C5—C6	108.96 (18)	C19—C20—C15	112.34 (19)
N1—C5—C10	110.67 (18)	O3N—N1N—O1N	121.5 (2)

C6—C5—C10	111.80 (19)	O3N—N1N—O2N	121.2 (2)
C5—C6—C7	113.14 (19)	O1N—N1N—O2N	117.2 (2)
C6—C7—C8	110.9 (2)	O4N—N2N—O5N	121.2 (3)
C9—C8—C7	111.7 (2)	O4N—N2N—O6N	120.4 (3)
C8—C9—C10	113.9 (2)	O5N—N2N—O6N	118.4 (2)
N2—C10—C9	108.6 (2)	O8N—N3N—O9N	120.9 (3)
N2—C10—C5	110.01 (18)	O8N—N3N—O7N	121.9 (3)
C9—C10—C5	112.33 (19)	O9N—N3N—O7N	117.2 (3)
C13—C12—N2	109.99 (18)	O11N—N4N—O12N	121.3 (2)
C13—C12—C11	112.6 (2)	O11N—N4N—O10N	121.4 (2)
N2—C12—C11	106.65 (19)	O12N—N4N—O10N	117.3 (2)
C12—C13—C14	109.62 (19)	H1O1—O1W—H2O1	107 (3)
N3—C14—C13	112.86 (19)	H1O2—O2W—H2O2	115 (3)

Within the tetraprotonated amine unit $[H_4L]^{4+}$, the C–C and N–C bond lengths are varied from 1.517 (3) to 1.541 (3) Å and from 1.500 (3) to 1.522 (3) Å, respectively. The range of N–C–C and C–N–C angles is 106.65 (19) to 112.86 (19)° and 117.94 (17) to 119.78 (19)°, respectively. The bond lengths and angles within the $[H_4L]^{4+}$ tetracation are comparable to those found in free ligand or dication in $(L)\cdot 2(C_{10}H_7CH_2OH)$, $(L)\cdot 2(NO_2OH)$, $[H_2L](SO_4)\cdot 2CH_3OH$, $[H_2L](ClO_4)_2$, $[H_2L]Br_2\cdot 2H_2O$. Generally, the N–C bond lengths in the exodentate conformation are longer than those in neutral macrocycle L and $[H_2L]^{2+}$ dication with an endodentate conformation. The N–O bond distances in the trigonal planar NO_3^- counter anion varied from 1.215(4) to 1.259(4) Å, and the O–N–O bond angles varied from 117.2(2)° to 121.9(3)°. The distorted geometry of the NO_3^- anion undoubtedly results from its involvement in hydrogen-bonding interactions with the organic cations and water molecules.

Extensive O–H···O, N–H···O, N–H···N and C–H···O hydrogen-bonding interactions occur in the crystal structure. The crystal packing diagram along the *c*-axis of 1 is shown in Fig. 7. Two water molecules are linked to the organic $[H_4L]^{4+}$ cation via N–H···O hydrogen bonds, whereas two of the four NO_3^- anions are directly linked to the organic $[H_4L]^{4+}$ cation via N–H···O and C–H···O hydrogen bonding interactions, and the remaining two NO_3^- anions are linked only to the water molecules via O–H···O hydrogen bonds. (Figs. 1 & 2). The extensive array of these contacts generates a three-dimensional network structure and these hydrogen-bonding interactions help to stabilize the crystal structure. Further distances and symmetry codes are given in Table 3. < Figure 3> <Table 3>

Table 3: Hydrogen bonds for 1 (Å and °)

D—H···A	D—H	H···A	D···A	D—H···A
N1—H1A···O9N^{i}	0.90	2.03	2.915 (3)	167.1
N1—H1B···O2W	0.90	1.87	2.751 (3)	165.0
N2—H2A···N1N^{ii}	0.90	2.54	3.431 (3)	169.5
N2—H2A···O1N^{ii}	0.90	2.21	2.966 (3)	141.0
N2—H2A···O2N^{ii}	0.90	2.13	2.988 (3)	159.1
N2—H2B···O10N	0.90	2.00	2.850 (3)	156.1
N3—H3A···N2N^{iii}	0.90	2.59	3.473 (3)	165.3
N3—H3A···O5N^{iii}	0.90	2.46	3.184 (3)	137.6
N3—H3A···O6N^{iii}	0.90	2.00	2.880 (3)	165.1
N3—H3B···O1W	0.90	1.92	2.747 (3)	152.9
N4—H4A···O1N	0.90	2.00	2.834 (3)	154.5
N4—H4B···N4N^{iv}	0.90	2.55	3.439 (3)	169.4
N4—H4B···O10N^{iv}	0.90	2.18	2.951 (3)	143.2
N4—H4B···O12N^{iv}	0.90	2.18	3.019 (3)	155.5
C1—H1C···O4N^{i}	0.97	2.55	3.296 (4)	133.8
C1—H1D···O1N	0.97	2.53	3.285 (4)	134.4
C2—H2···O2N^{v}	0.99	2.41	3.361 (3)	159.8
C3—H3C···O11N^{vi}	0.98	2.59	3.364 (4)	135.5
C4—H4D···O3N^{v}	0.98	2.57	3.484 (4)	155.7
C6—H6A···O4N^{vii}	0.98	2.48	3.213 (3)	131.4
C9—H9A···O9N^{i}	0.98	2.58	3.391 (4)	140.3
C10—H10···O3N^{v}	0.99	2.55	3.531 (3)	171.7
C11—H11A···O8N	0.97	2.53	3.354 (4)	142.5
C11—H11C···O10N	0.97	2.57	3.360 (4)	138.2
C12—H12···O12N^{vi}	0.99	2.40	3.386 (3)	171.3
C13—H13B···O5N^{iii}	0.98	2.50	3.213 (3)	129.6
C14—H14A···O11N^{vi}	0.98	2.51	3.411 (3)	152.1
C16—H16A···O6N^{iii}	0.98	2.47	3.280 (4)	139.5
C20—H20···O11N^{vi}	0.99	2.55	3.530 (3)	172.8
O1W—H1O1···O5N	0.917 (14)	1.932 (17)	2.825 (4)	164 (4)
O1W—H2O1···O7N	0.917 (14)	1.923 (14)	2.839 (4)	178 (4)

O2W—H1O2···N2N^{vii}	0.904 (14)	2.53 (2)	3.385 (4)	157 (4)
O2W—H1O2···O4N^{vii}	0.904 (14)	2.42 (4)	3.070 (4)	129 (4)
O2W—H1O2···O6N^{vii}	0.904 (14)	2.020 (16)	2.919 (3)	173 (4)
O2W—H2O2···O8N^{vi}	0.913 (14)	2.12 (3)	2.956 (5)	151 (4)

Symmetry codes: (i) *x*−1, *y*, *z*; (ii) *x*, *y*−1, *z*; (iii) −*x*+1, *y*−1/2, −*z*; (iv) *x*, *y*+1, *z*; (v) −*x*, *y*−1/2, −*z*; (vi) −*x*+1, *y*+1/2, −*z*+1; (vii) −*x*+1, *y*−1/2, −*z*+1.

2. Hirshfeld surface analysis

Hirshfeld surface (HS) and 2D fingerprint plot were drawn using CrystalExplorer. HS analysis is a valuable tool for visualizing and quantifying intermolecular interactions in a crystal structure, providing insight into how molecules pack together in the solid state. The most widely used color scheme of HS, where red indicates shorter contact (stronger interaction), white indicates van der Waals separation, and blue indicates longer contact (weaker interaction). Fig. 4 shows the HS of 1 mapped over d_{norm} function, where it is evident from the bright-red spots appearing near the O atoms of water molecules and nitrate anions that these atoms play a significant role in the molecular packing.

< Figure 4> 2D fingerprint plots are illustrated in Fig. 5 with the percentage contributions of the main contacts to the total HS. < Figure 5> The fingerprint plots can be decomposed to highlight particular atoms pair close contacts. Globally, the highest contribution of total HS is attributed to H···O/O···H interactions with 63.8%. Contributions from the H···O/O···H contacts appear as a pair of sharp spikes characteristic of strong hydrogen bonding interactions. There are actually three types of hydrogen bonds in the crystal structure: O—H···O, N–H···O and C–H···O (Table 2, Fig. 3). The H···H contacts are the second most frequent interactions (30.9%) due to the abundance of hydrogen on the molecular surface. The N···H interactions constitute only 3.2% of the contacts. Consequently, the contact analysis for this compound suggests that the three types of hydrogen bonds are the driving force in molecular arrangement and crystal packing formation.

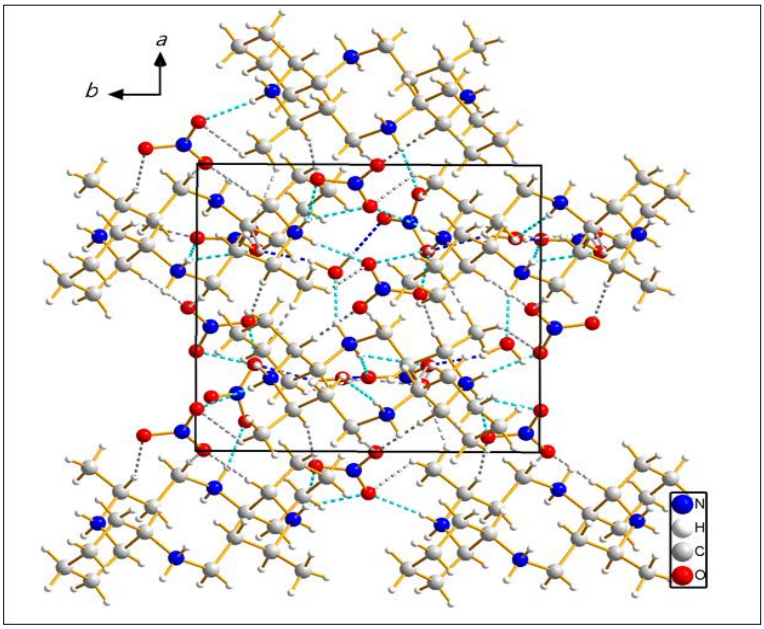

Fig 3: The crystal packing of 1, viewed down the *c* axis. Dashed lines represent N–H···O (blue), N–H···Cl (pink) and O–H···Cl (cyan) hydrogen bonding interactions, respectively. H atoms bound to C have been omitted

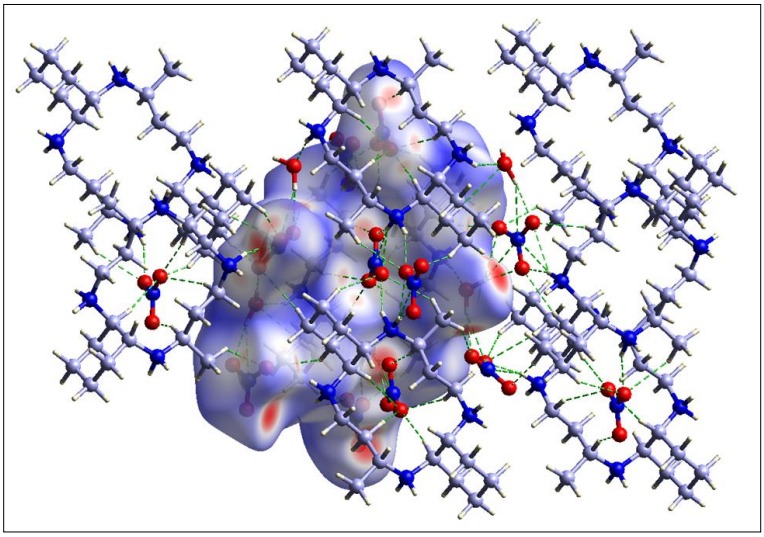

Fig 4: HS plot of 1 mapped with d_{norm} function, where the dashed lines represent hydrogen bonds and close contacts

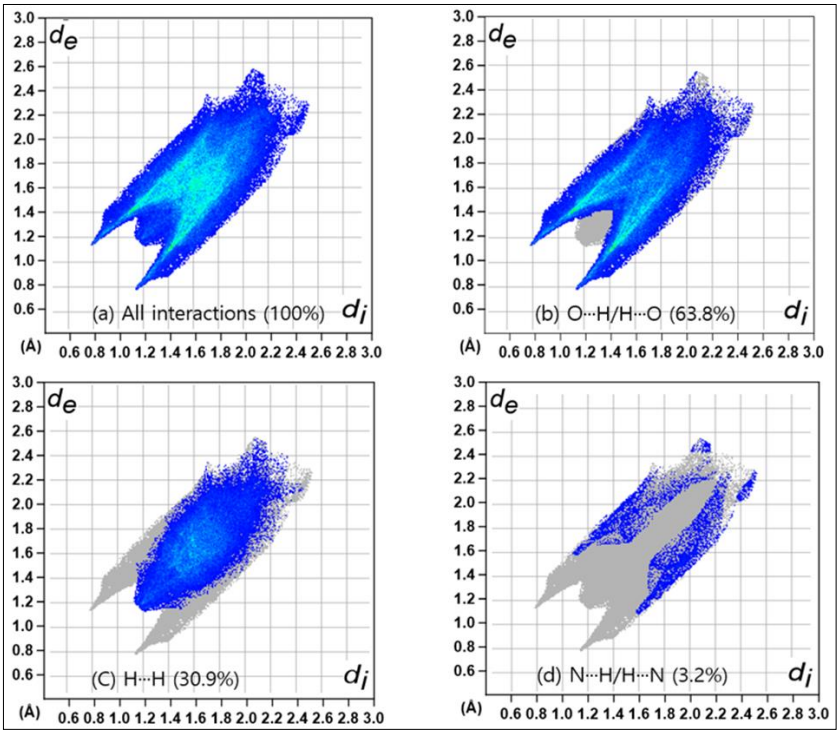

Fig 5: 2D fingerprint maps of 1, showing (a) all interactions, and delineated into (b) O···H/H···O, (c) H···H and (d) N···H /H···N interactions

Additional smaller contributions provided by other interatomic contacts to the HS are as follows: O···O (1.7%) and N···O (0.4%). All interactions observed in 1 are summarized in Table 4. The small percentage contributions from the remaining interatomic contacts are summarized in Table 3. The large number of H···O/O···H and H···H contacts suggest that hydrogen bonding and van der Waals interactions play the major roles in the crystal packing, which is consistent with the crystal packing topology.
<Table 4>

Table 4: Summary of all contacts and their contributions to the HS

Type of contact	Contribution (%)
H···O	63.8
H···H	30.9
H···N	3.2
O···O	1.7
N···O	0.4

Conclusion

The newly prepared organic salt, $[C_{20}H_{44}N_4](NO_3)_4{\cdot}2H_2O$ (1),was characterized by elemental analysis and single-crystal X-ray diffraction analysis. The asymmetric part of 1 consists of one full organic $[H_4L]^{4+}$ cation, four nitrate anions, and two water molecules. The tetraprotonated organic cation adopts the (3,4,3,4)-*A* exodentate conformation as a consequence of strong intermolecular hydrogen bonds between nitrate anions and hydrated water molecules. The N–H···O, C–H···O and O—H···O hydrogen bonds interconnect macrocyclic tetracations with water molecules and nitrate anions, giving rise to a three-dimensional network of molecules. These hydrogen-bonding interactions help to stabilize the crystal structure. HS analysis and 2D fingerprint plots also revealed that the structure in the solid-state is mainly dominated by O···H/H···O (63.8%), H···H (30.9%), and N···H/H···N (3.2%) contacts.

Funding

The X-ray crystallography experiment at the PLS-II BL2D-SMC beamline was supported in part by MSIT and POSTECH.

Supplementary Material

Full crystallographic data have been deposited with the Cambridge Crystallographic Data Centre, CCDC No. 2519884. Copies of this information may be obtained free of charge from The Director, CCDC, 12 Union Road, Cambridge CB2 1EZ, UK (fax: +44-1223-336-033; e-mail: deposit@ccdc.cam.ac.uk or www: http://www.ccdc.cam.ac.uk).

References

1. Valks GC, McRobbie G, Lewis EA, Hubin TJ, Hunter TM, Sadler PJ, et al. Configurationally restricted bismacrocyclic CXCR4 receptor antagonists. J. Med. Chem,2006:49:6162-6165.
2. Ronconi L, Sadler PJ. Using coordination chemistry to design new medicines. Coord. Chem. Rev,2007:251:1633-1648.
3. De Clercq E. Highlights in the discovery of antiviral drugs: A personal retrospective. J. Med. Chem. 2010, 53. 1438-1450.
4. Ross A, Choi JH, Hunter TM, Pannecouque C, Moggach SA, Parsons S, et al. Zinc(II) complexes of constrained antiviral macrocycles. Dalton Trans,2012:41:6408-6418.
5. Kang SG, Kweon JK, Jung SK. Synthesis of new tetraaza macrocyclic ligands with cyclohexane ring and their Ni(II) and Cu(II) complexes. Bull. Korean Chem. Soc,1991:12:483-487.
6. Meyer M, Dahaoui-Gindrey V, Lecomte C, Guilard R. Conformations and coordination schemes of carboxylate and carbamoyl derivatives of the tetraazamacrocycles cyclen and cyclam, and the

relation to their protonation states. Coord. Chem. Rev,1998:178–180:1313–1405.
7. Moon D, Jeon J, Choi JH. Two exodentate conformations, spectroscopic properties, and Hirshfeld surface analysis of new macrocyclic compounds with tetrabromide and tetraperchlorate. J. Mol. Struct,2021:1243:130790.
8. Choi JH, Subhan MA, Ryoo KS, Ng SW. 3,14-dimethyl-2,6,13,17-tetraazatricyclo(16.4.0.07,12)docosane (naphthalen-1-yl)methanol. Acta Crystallogr,2012:E68:o102.
9. Moon D, Jeon S, Ryoo KS, Choi JH. Synthesis, Crystal Structure and Hirshfeld Surface Analysis of 3,14-dimethyl-2,6,13,17-tetraazatricyclo(16.4.0.07,12)docosane-2-(nitric acid). Asian J. Chem,2020:32:697-702.
10. White F, Sadler PJ, Melchart M. CSD Communication. 2015. CCDC 1408165.
11. Moon D, Jeon S, Choi JH. Crystal structure of 3,14-dimethyl-2,13-diaza-6,17-diazoniatricyclo(16.4.0.07,12)docosane bis(perchlorate) from synchrotron X-ray data. Acta Crystallogr,2021:E77:551-554.
12. Moon D, Jeon S, Choi JH. Crystal structure, endo/exodentate conformations, spectroscopic properties, and Hirshfeld surface analysis of two constrained cyclam compounds with bromides and hydrates. J. Mol. Struct,2021:1232:130011.
13. Moon D, Choi JH. Crystal structure of 3,14-dimethyl-2,6,13,17-tetraazoniatricyclo(16.4.0.07,12)docosane tetrachloride tetrahydrate from synchrotron X-ray data. Acta Crystallogr,2018:E74:1039-1041.
14. Shin JW, Eom K, Moon D. BL2D-SMC, the supramolecular crystallography beamline at the Pohang Light Source II, Korea. J. Synchrotron Rad,2016:23:369-373.
15. Otwinowski Z, Borek D, Majewski W, Minor W. Multiparametric scaling of diffraction intensities. Acta Crystallogr,2003:A59:228-234.
16. Sheldrick GM. SHELXT-Integrated space-group and crystal-structure determination. Acta Crystallogr,2015:A71:3-8.
17. Sheldrick GM. Crystal structure refinement with SHELXL. Acta Crystallogr,2015:C71:3-8.
18. Brandenburg K, Putz H. DIAMOND-5, University of Bonn, Germany, 2023.
19. Moon D, Choi JH. Crystal structure of 1,4,8,11-tetramethyl-1,4,8,11-tetraazoniacyclotetradecane bis[chloridochromate(VI)]dichloride from synchrotron X-ray data. Acta Crystallogr,2020:E76:523–526.
20. Moon D, Choi JH. Crystal structure of 1,4,8,11-tetramethyl-1,4,8,11-tetraazoniacyclotetradecane bis(perchlorate) dichloride from synchrotron X-ray data. Acta Crystallogr,2020:E76:324–327.
21. Moon D, Choi JH. Crystal structure of 1,4,8,11-tetraazoniacyclotetradecanebis(dichromate) monohydrate from synchrotron data. Acta Crystallogr,2017:E73:755–758.
22. McKinnon JJ, Jayatilaka D, Spackman MA. Towards quantitative analysis of intermolecular interactions with Hirshfeld surfaces. Chem. Commun, 2007, 3814-3816.
23. Spackman MA, McKinnon JJ. Fingerprinting intermolecular interactions in molecular crystals. CrystEngComm,2002:4:378-392.
24. Spackman PR, Turner MJ, McKinnon JJ, Wolff SK, Grimwood DJ, Jayatilaka D, et al. CrystalExplorer: a program for Hirshfeld surface analysis, visualization and quantitative analysis of molecular crystals. J. Appl. Cryst,2021:54:1006-1061.
25. Aree T, Hong YP, Choi JH. Crystal structures, spectroscopic characterization, and Hirshfeld surface analyses of three constrained cyclam compounds with perchlorate counteranions. J. Mol.Struct,2018:1163:86-93.
26. Moon D, Tanaka S, Akitsu T, Choi JH. Molecular structure, spectroscopic properties,and Hirshfeld surface analysis of chlorobis(N-methyl-1,3-propanediamine)copper(II) tetrafluoroborate and azidobis(2,2-dimethyl-1,3-propanediamine)copper(II) azide. J. Mol. Struct,2018:1154:338-347.
27. Jeon S, Moncol J, Mazúr M, Valko M, Choi JH. Synthesis, crystal structure, spectroscopic Properties, and Hirshfeld surface analysis of diaqua[3,14-dimethyl-2,6,13,17-tetraazatricyclo(16.4.0.07,12)docosane]copper(II) dibromide. Crystals,2019:9:336.
28. Moon D, Choi JH. Synthesis, crystal structure, infrared spectroscopy, and Hirshfeld surface analysis of cis-(thiocyanato)(1,4,8,11-tetraazacyclotetradecane)chromium(III)(μ-1,3-thiocyanato)trichloridozincate. J. Coord. Chem,2021:74:969-981.
29. Moon D, Jeon S, Mazúr M, Valko M, Choi JH. Structural characterization, spectroscopic properties, and Hirshfeld surface analysis of two copper(II) complexes with 3,14-dimethyl and 3,14-diethyl-2,6,13,17-diazadiazoniatricyclo[16.4.0.07,12]docosa-2,13-diene. J. Mol. Struct,2021:1229:129897.